TECHNICAL MEMORANDUM

533

Impact of SSM/I Observations related to Moisture, Clouds and Precipitation on Global NWP Forecast Skill

Graeme Kelly, Peter Bauer, Alan J. Geer, Philippe Lopez, and Jean-Noël Thépaut

Research Department

European Centre for Medium-Range Weather Forecasts, UK

Submitted for publication in Monthly Weather Review

August 2007

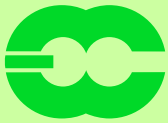

European Centre for Medium-Range Weather Forecasts
Europäisches Zentrum für mittelfristige Wettervorhersage
Centre européen pour les prévisions météorologiques à moyen terme

Series: ECMWF Technical Memoranda

A full list of ECMWF Publications can be found on our web site under:
http://www.ecmwf.int/publications/

Contact: library@ecmwf.int

European Centre for Medium-Range Weather Forecasts
Shinfield Park, Reading, RG2 9AX, England

Abstract

This paper presents the results from Observing System Experiments with the current ECMWF data assimilation and modeling system for quantifying the impact on both analysis and forecast quality of SSM/I observations sensitive to moisture and clouds as well as precipitation. SSM/I radiances have been assimilated operationally in clear-sky areas for many years and since June 2005 in cloud and rain-affected areas too. This paper examines experiments set up such that clear-sky and rain-affected observations were either added to a poor baseline observing system configuration or withdrawn from the full system. Experiment duration was 10 weeks of which the first 14 days were excluded from the evaluation to allow for model spin-up.

The basic analysis impact evaluation demonstrates that both clear-sky and rain-affected observations account for the bulk correction of moisture in the ECMWF analysis. The rain-affected data exhibits a stronger interaction with vertical motion than the clear-sky data through convection and therefore affects tropical convergence and high cloud cover.

SSM/I data adds 1 day of forecast skill over the first 48 hours when evaluated in addition to a poor observing system. In the Tropics, the rain-affected data contributes more skill to the moisture forecast than the clear-sky data at 700 hPa and above. In the Northern and Southern hemisphere, the effect is generally weaker and slightly in favour of clear-sky observations. A similar performance can be seen with respect to wind vector forecast skill that indicates the connection between moisture analysis and vertical motions.

1 Introduction

Clouds and precipitation strongly affect the global hydrology and energy cycles, mainly through the interaction of solar and infrared radiation with cloud droplets and the release of latent heat in precipitation development. The accurate representation of clouds and precipitation in numerical weather prediction (NWP) systems is crucial for daily forecasting, in particular in case of extreme weather conditions. Many catastrophic weather events are associated with extreme winds but also extreme precipitation. On climatological time scales, even droughts must be considered as weather extremes through the systematic and long-term anomalous lack of precipitation.

About 3 million satellite observations are actively assimilated per 12-hour analysis cycle in the four-dimensional variational (4D-Var) assimilation systen at ECMWF (model cycle 30R1, June 2006) that is about 98% of the total data volume. In general, radiance observations are only assimilated in clear skies. This is because the forward modelling of radiance signatures of clouds and precipitation is much less accurate than in clear skies. Most crucially affected are observations that are sensitive to the mid to lower troposphere and, in particular, to atmospheric moisture. Observing system experiments (Andersson et al. 2007) suggest that the most dominant humidity observations in the analysis originate from Special Sensor Microwave / Imager (SSM/I) and Advanced Microwave Sounding Unit (AMSU-B). Over land, radiosondes, ground-based stations and AMSU-B observations dominate. In the upper troposphere, also infrared sounding channels from the High-resolution Infra-Red Sounder (HIRS), the Atmospheric Infra-Red Sounder (AIRS) and radiometers onboard geostationary satellites contribute signifi cant information on humidity to the atmospheric analysis.

When global rainfall observations from the Tropical Rainfall Measuring Mission (TRMM) Precipitation Radar (PR) are analyzed, the main driver for regional differences in precipitation amount is rainfall occurrence rather than rain intensity (Kidd, pers. communication). In the tropical convergence zones, rainfall occurs at a rate of 8% or more while in areas with larger-scale precipitation systems rainfall occurrence is of the order of 5%. These values apply only to the original spatial resolution of the PR, which is 4 km. If they are averaged to the current approximate spatial resolution of the ECMWF model, rainfall occurence reaches about 25% and more in areas where convective precipitation regimes are dominant. This means that for data assimilation systems that

screen out precipitation-affected observations a number of undesirable effects occur. First, in particular over Southern Hemisphere oceans, large areas are not well covered by observations that are sensitive to humidity so that the moisture analysis is mainly constrained by the model background (i.e. short-range forecast) in each analysis. Secondly, as seen in the ECMWF Re-analysis (ERA-40, Uppala et al 2005) an underestimation of atmospheric moisture by the model together with positive humidity increments from observations led to an imbalance in the hydrological budget that was accompanied by precipitation spin-up. Recently, improvements in model physics and the data assimilation system helped to substantially reduce these problems (Andersson et al. 2005).

Apart from general predictability issues with regard to clouds and precipitation, the forecasting of processes involving the hydrological cycle is generally much less accurate than that of dynamical fields. This is mainly because of the less accurate moist physics parameterizations but also because moist processes strongly depend on less well predicted dynamical parameters like vertical wind.

Despite the underlying problems, both the continuous availability of accurate moisture observations and the progress in physical modelling and data assimilation system development pave the way for the use of cloud and precipitation affected observations in modern NWP systems. While these new observations represent greater technical challenges a substantial benefit for NWP skill improvement can be expected due to the lack of competing observations in cloudy areas over large parts of the globe.

Since weather system development at lower latitudes is more dominated by convection and less by large-scale dynamics, the first attempts to produce better moist initial conditions for model forecasts were made through adjustments of diabatic heating using infrared sounder data (e.g.Heckley et al. 1990) and moisture initialization and heating adjustments from outgoing longwave radiation observations (OLR; Puri and Miller 1990). The development of more complex physical initialization schemes included the use of OLR and retrieved surface rain-rates from satellite data to constrain surface fluxes, moisture flux profiles and their feedback with convection and radiation (Krishnamurti et al. 1984, Krishnamurti and Bedi 1996).

The advent of variational data assimilation schemes involving adjoint techniques initiated the employment of more complex and more consistent model physics in model initialization using cloud and precipitation observations. Apart from a number of experimental and case-study oriented methods (e.g. Zupanski and Mesinger 1995, Zou and Kuo 1996, Tsuyuki 1997), only very few implementations in operational forecasting systems have succeeded so far. This is because of a number of fundamental problems associated with the assimilation of rain-affected observations, some of which can only be pragmatically solved (Errico et al. 2007).

The ECMWF version of rainfall assimilation represents a unique step forward in that it is based on the variational assimilation of passive microwave radiance observations and that it performs the assimilation with an operational 4D-Var system on a global scale (Bauer et al. 2006a, Bauer et al. 2006b). The current operational version is a preparatory step towards the implementation of a direct 4D-Var assimilation of rain affected radiances. The system has worked successfuly since its operational implementation in June 2005 and has undergone several upgrades.

This paper presents the first systematic performance analysis of such a system in global operational applications and is based on Observing System Experiments (OSEs) using the current ECMWF data assimilation and forecasting system. The rain assimilation system is briefly introduced in Section 2 together with the description of the experimental set-up. The forecast performance is presented in Section 3 and conclusions are drawn in Section 4.

2 Observing System Experiments

2.1 Data Assimilation System

ECMWF employs a 4D-Var data assimilation system that is run in two different analysis suites twice per day. One suite runs 4D-Var over a 12-hour window and produces analyses at 00 and 12 UTC, respectively. From these, short-range forecasts are generated that serve as model first-guess estimates of the atmospheric state for the second suite. The second suite runs again two analyses per day over 6-hour windows centred at 00 and 12 UTC, respectively. The second suite initializes the global medium-range forecasts. Details of the 4D-Var system can be found in Courtier et al. (1994) and Rabier et al. (1997) while the latest analysis suite set-up is described by Haseler (2004).

Originally, clear-sky SSM/I data was used in a one-dimensional variational retrieval of total column water vapour and near-surface wind speed in the ECMWF system (Phalippou et al. 1996, Gérard and Saunders 1999) that was later replaced by the direct radiance assimilation in 4D-Var (Bauer et al. 2002). The rain assimilation system was introduced in 2005 and is based on a 1D+4D-Var assimilation of passive microwave radiance measurements from the Special Sensor Microwave / Imager (SSM/I) onboard the Defense Meteorological Satellite Program (DMSP) platforms. 1D+4D-Var refers to a one-dimensional variational retrieval (1D-Var) of total column water vapour (*TCWV*) in the presence of clouds and precipitation from SSM/I radiances followed by a 4D-Var assimilation of *TCWV* in the full system. Per analysis cycle, i.e. 12-hour window, about 50,000 SSM/I observations over global oceans are assimilated. Details of 1D+4D-Var design and implementation are given by Bauer et al. (2006a, b).

Currently, the high-resolution analyses and forecasts are produced at 25 km spatial resolution (spectral wavenumber cut-off at 799) and on 91 model levels. For the sake of efficiency, the Observing System Experiments (OSEs) presented in this paper were run at lower resolution, i.e. 40 km (spectral wavenumber cut-off at 511) and on 60 model levels. In the minimization, the spatial resolution is increased in successive inner loops (minimization steps) from a wavenumber cut-off at 95 to 159 (e.g. Tremolet 2004).

A large number of observations is currently assimilated at ECMWF, comprising conventional and, for the largest part, satellite observations. Conventional observations currently assimilated in the system include radiosondes, pilots and wind profilers, synoptical observations, data from ships and buoys (moored and drifters), as well as aircrafts including reports during ascent/descent. Satellite observations include Atmospheric Motion Vectors (AMVs) derived from geostationary platform data (Meteosat-5/8, GOES-9/10/12) and low-Earth orbiting satellites (MODIS onboard TERRA and AQUA); clear-sky water vapour radiances from Meteosat-5/8 and GOES-9/10/12, infrared radiances from NOAA-17 (HIRS) and AQUA (AIRS), microwave radiances from NOAA-15 (AMSU-A), NOAA-16 (AMSU-A and AMSU-B), NOAA-17 (AMSU-B),NOAA-18 (AMSU-A, MHS), AQUA (AMSU-A) and DMSP F-13/14/15 (SSM/I); sea surface winds from scatterometers onboard QuikScat and ERS-2; ozone products from NOAA-16 (SBUV) and ENVISAT (SCIAMACHY).

2.2 Experiments

At its meeting at ECMWF on the 3rd of May 2003, the European Meteorological Network (EUMETNET) Composite Observing System (EUCOS) Scientific Advisory Team discussed the need to investigate the interdependencies between the space-based and terrestrial components of the observing system. It was suggested that such an investigation could be based on a set of carefully designed OSEs. Studies should be designed so as to provide guidance on the future development of the terrestrial observing system in view of the increasing capabilities of the satellite observing systems provided by the meteorological space agencies (Andersson et al.

2004). The following experiments were designed accordingly and in agreement with EUMETSAT.

All experiments were run for the period of June 1 - August 15, 2006. The initial 14-day period was excluded from the verification to allow for the system to spin-up and to eliminate the effect of the operational model that initialized the first analysis. To avoid strong interaction of model climate change with the recently introduced variational bias correction (VarBC; Dee 2005, Auligné et al. 2007), in particular in the experiments with poor observing systems, VarBC was only activated for the initial 14-day period and bias-corrections were frozen for the remaining time. In general, the 4D-Var system is based on the assumption that the differences between observations and model-simulated parameters are not affected by biases and that their probability distributions have Gaussian shapes so that error properties can be described by error covariance statistics. All following results refer to the period 15/06-15/08/2007.

Since both observations and model contain biases due to technical deficiencies as well as model inaccuracies, observation system characteristics as well as model variables are used as predictors in bias-correction schemes. The basic principle of VarBC is to include biases in the 4D-Var control vector such that the analysis derives an optimal model state that also minimizes biases. VarBC may also be affected by spin-up if the observation system is drastically changed, and this is certainly the case in the OSEs presented here. The time for spin-up depends on the sensor and which parameter it is sensitive to. For moisture related observations, the spin-up takes a few days while for atmospheric temperature and in the middle and higher atmosphere the spin-up evolution can be much slower. To avoid such effects no bias-predictor spin-up was allowed after the initial 14-day warm-up period.

The following experiments have been performed:

1. *BL*: A baseline configuration that includes all conventional observations as well as AMSU-A radiance observations from NOAA-16. The latter was found to be important because the sparsity of conventional observations over the Southern hemisphere and Tropics produces too poor analyses of the mass field otherwise.

2. *CTRL*: A control run with the full operational observation system.

3. $BL + RAIN$: Baseline + SSM/I 1D+4D-Var rain observations from DMSP-13/14/15.

4. $BL + CLEAR$: Baseline + SSM/I clear-sky radiance observations from DMSP-13/14/15.

5. $BL + RAIN + CLEAR$: Baseline + SSM/I clear-sky and rain affected observations.

6. $CTRL - RAIN$: Full operational observation system but SSM/I 1D+4D-Var rain observations withdrawn.

7. $CTRL - CLEAR$: Full operational observation system but SSM/I clear-sky radiance observations withdrawn.

This set-up allows the evaluation of the performance of data addition and denial on forecast skill. Given the rather well constrained operational analysis and the rather poor baseline configuration, the denial of data will exhibit much less impact than the addition of data. However, due to the non-linear response of the system to data addition and denial a consistent evaluation at both ends of the scale is possible. The assessment of the individual and combined contribution of SSM/I clear-sky and rain-affected observations helps understanding the degree of redundancy and complementarity between both observation types.

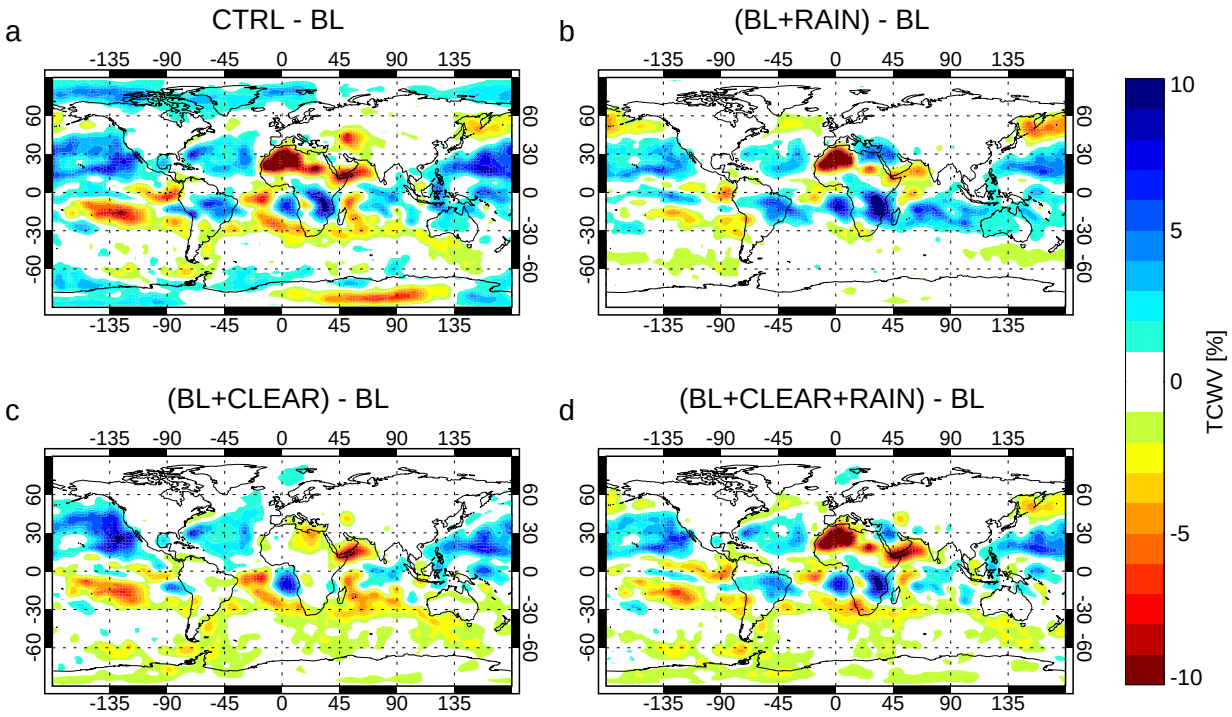

Figure 1: Mean analysis difference for TCWV as % of TCWV content of BL experiment: CTRL minus BL (a), BL + RAIN minus BL (b), BL + CLEAR minus BL (c), BL + CLEAR + RAIN minus BL (d).

3 Results

3.1 Analysis

3.1.1 Data addition experiments

The fundamental impact of clear-sky SSM/I observations on the lower tropospheric humidity analysis over oceans has been demonstrated by earlier OSEs with previous ECMWF model versions and the available observing systems at that time (Andersson et al. 2007). From these, Andersson et al. concluded that the SSM/I provides the strongest observational contribution to moisture below 500 hPa.

Above that level, sounder-type sensors with better sensitivity to middle and upper tropospheric moisture, such as the AMSU-B and the water-vapour sounding channels on the geostationary imagers, take over. However, the bulk of the total atmospheric moisture is located below 500 hPa, it is therefore fair to say that the *TCWV* analysis over oceans is mainly driven by SSM/I observations.

Figure 1a shows the mean analysis difference in *TCWV* between *CTRL* and *BL* (in % of *TCWV* from *BL*). Since SSM/I observations are only assimilated over oceans, the impact is small over large continental areas like North America and Eurasia. The SSM/I data tends to systematically moisten the largest part of the Northern hemispheric oceans at latitudes below 50 degrees. In the Southern hemisphere (winter hemisphere), the effect is reversed and focused on latitudes between the equator and 30 degrees South. Figures 1b-d demonstrate that both clear-sky and rain-affected SSM/I observations (i.e., $BL + RAIN$, $BL + CLEAR$, $BL + RAIN + CLEAR$) work very similarly on the *BL* moisture distribution. However, $BL + CLEAR$ seems to emphasize the moistening in

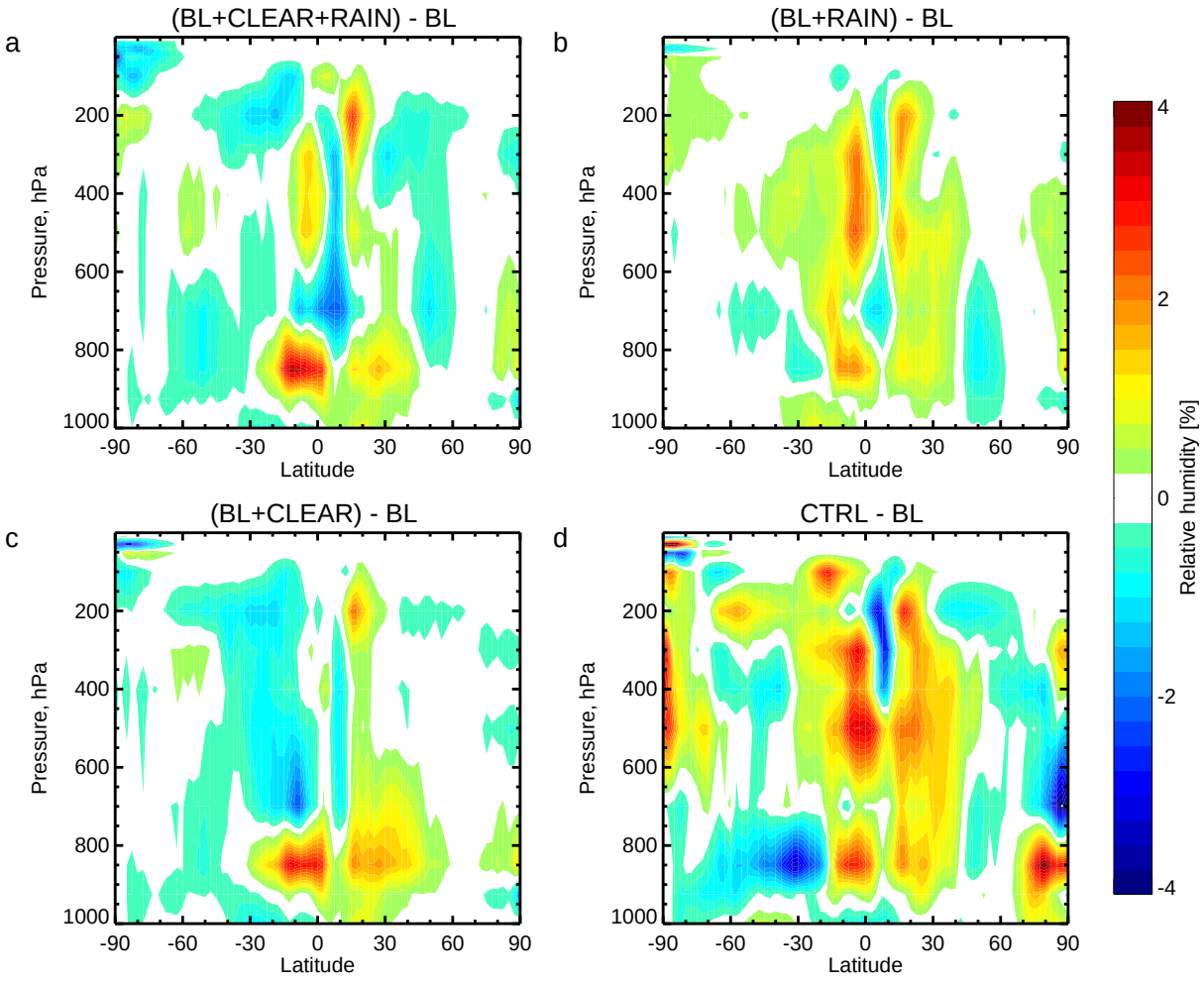

Figure 2: Zonal cross-sections of mean relative humidity analysis difference: BL + CLEAR + RAIN minus BL (a), BL + RAIN minus BL (b), BL + CLEAR minus BL (c), CTRL minus BL (d).

Northern oceans and the drying in Southern oceans while the rain assimilation tends towards more moistening in the Southern subtropical areas and drying in the Northern Pacific. The combined effect (Figure 1d) is very similar to the total effect of all observations (Figure 1a) highlighting the dominance of the SSM/I for the *TCWV* analysis.

One substantial difference between adding clear-sky or cloud/rain-affected observations to *BL* is the impact over land. Only *BL + CLEAR* minus *BL* (Figure 1c) does not show a substantial moisture analysis changes over land from the oceanic observations. Most likely, the reason is in the stronger impact of cloud/rain-affected observations on vertical motion and therefore on atmospheric circulation. In the Northern hemisphere summer, there is strong moisture advection from the central Atlantic into the Northern part of South America and from the Western Indian Ocean into Central Africa producing a maritime precipitation climate in these areas (Kållberg et al. 2005, Figure C3, page 36). This feature is amplified when cloud/rain-affected observations are added to *BL*. Over Northern Africa, the moisture flux is directed from the Eastern Mediterranean Sea into Egypt. The relative moisture increase in this area as well as over the Sahara from adding cloud/rain-affected observations, however, may not be considered significant because in this period atmospheric moisture contents reach their annual minimum so that relative increments may be substantial but absolute increments are small.

Figure 2 shows the zonal cross-sections of analysis differences for relative humidity, R, in %. The moistening with respect to BL from all other addition-experiments in the Northern hemispheric tropics and sub-tropics extends throughout the entire troposphere. $BL+CLEAR$ contributes a large part only just above the boundary layer near 850 hPa (roughly 1.5 km altitude) while $BL+RAIN$ intensifies the vertical moisture transport through convection. The vertical profile of increments is mainly driven by the shape of the humidity control variable background error standard deviation function. This peaks near that level and drops off rather sharply towards the surface and more smoothly towards the top of the atmosphere. The weak drying in the Southern hemisphere is mainly produced by clear-sky observations and is weakened by the rain assimilation, mainly at levels above the boundary layer. $CTRL$ is much drier than BL in much of the tropics as seen in Figure 2d. The combined effect of $CLEAR$ and $RAIN$ shown in Figure 2a does not feature such extensive drying. This must therefore be the product of other observations sensitive to moisture.

3.1.2 Data denial experiments

The effect on the average moisture analysis changes rather dramatically when SSM/I observations are withdrawn from $CTRL$. While the previous results were related to baseline experiments without moisture-sensitive observations, the denial experiments refer to a full observing system where only SSM/I data has been taken out. Figure 3 shows the effect on TCWV of the denial of rain-affected and clear-sky observations as differences with respect to $CTRL$. The differences have been normalized by $CTRL$ and are presented in units of %.

As already shown in Bauer et al. (2006b), large areas of systematic drying are produced when rain-affected SSM/I observations are assimilated (Figure 3a). These patterns are statistically significant over large parts of the summer hemisphere with maximum values of 5-10% in the Northern Pacific. The only large-scale moistening is found in the subtropical subsidence zones South of the ITCZ. These moisture differences associated with mean sea-level pressure (MSLP) and lower level divergence changes in the analysis as also shown by Bauer et al. (2006b). Drying coincides with MSLP increase and divergence while moistening produces a MSLP decrease and convergence. However, only little interaction with vertical motion could be identified. Both short-range forecasts of convective available potential energy (CAPE) and precipitation did not seem to pick up the initial moisture analysis signal. Only high cloud cover was found to systematically decrease (order 10-20%) along the ITCZ near 10-15 degrees North along with the TCWV reduction.

When clear-sky SSM/I data is withdrawn (Figure 3b), TCWV analysis patterns show a different behaviour with patchy structures in the Northern hemisphere and predominantly dryer analyses over the Southern hemisphere oceans. These areas coincide with generally dry air masses and little cloud and precipitation occurrence at this time of the year. Evidently, no direct link between TCWV changes and divergence, clouds, instability or precipitation could be found. It must be concluded that both observation types mainly work on systematic model biases that are related to areas where moist diabatic processes dominate ($RAIN$) or in areas well below saturation and with little cloud presence ($CLEAR$). The stronger impact of rain-affected observation on divergence indicates that, potentially, model biases are larger and that fewer observation types are available in these areas. The lack of direct impact of the moisture analysis on cloudiness and precipitation suggests that the physics parameterizations dissipate the signal rather quickly.

3.2 Forecast

The first forecast evaluation is again performed for $TCWV$. Figure 4 shows the summary of global root-mean-square (RMS) forecast errors for all experiments until day 6. The RMS-errors are calculated by comparing the forecasts with the operational ECMWF analyses. Note that the operational system employs a higher spatial resolution and is based on two analyses, of which the first 12-hour 4D-Var assimilation is used to produce a

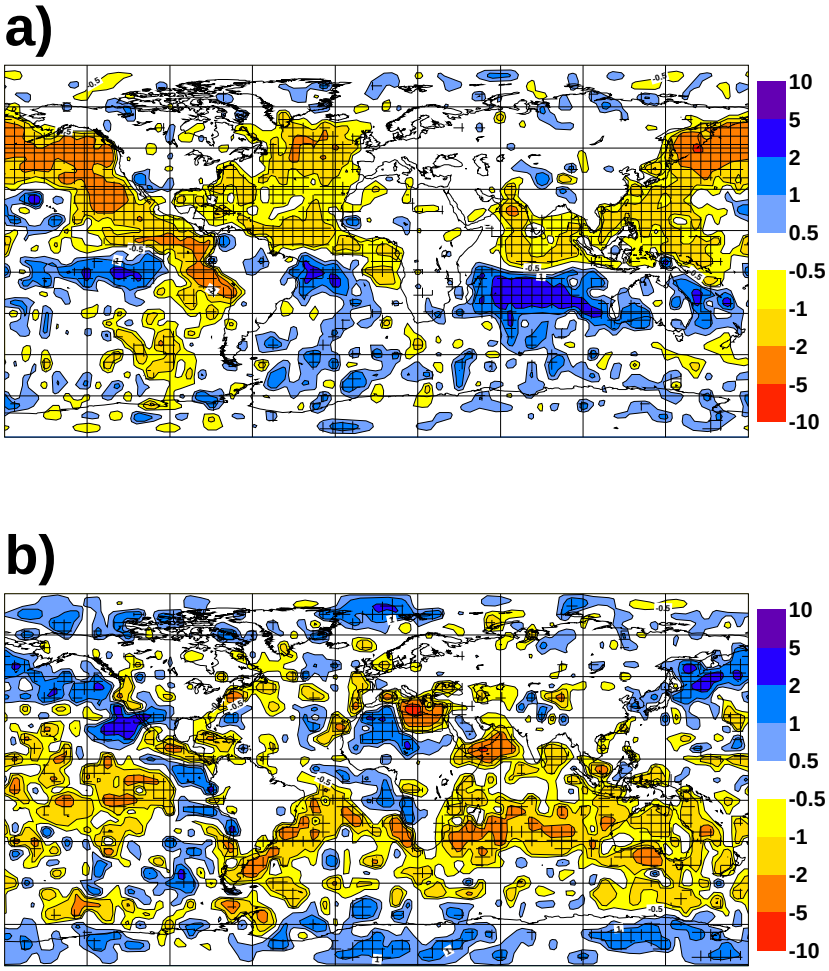

Figure 3: Mean relative analysis difference for TCWV (in %) CTRL minus CTRL – RAIN (a) and CTRL minus CTRL – CLEAR. Hatched areas indicate regions where the calculated differences reach 95% statistical significance.

short-range forecast as the first guess for the second assimilation which is based on a 6-hour 4D-Var assimilation. Only the latter is used to initialize the medium-range forecast. When evaluating forecasts against analyses, the choice of analysis can affect the results. The operational, rather than the *CTRL* analyses, were chosen for their relative independence from the OSE experiment configuration so as to avoid spuriously amplifying the apparent impact of the observing system.

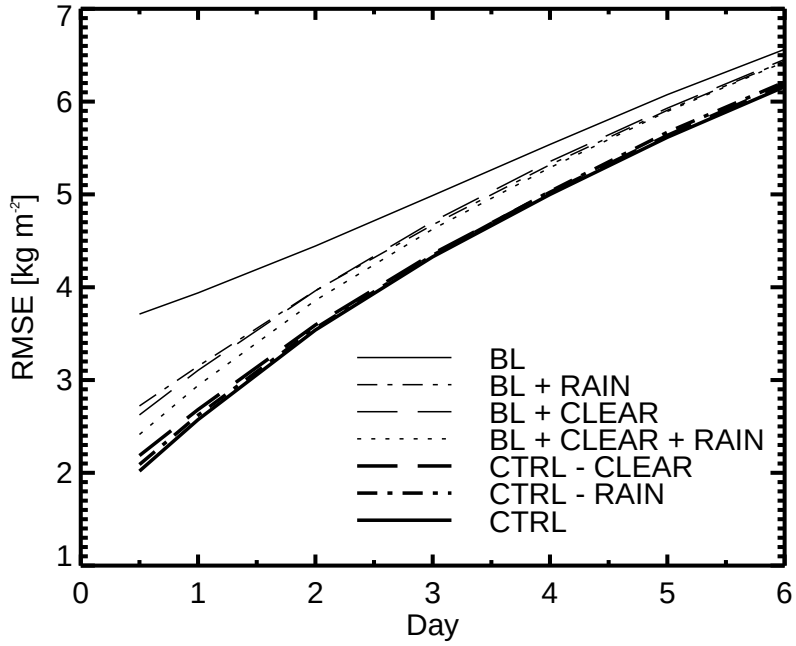

Figure 4: Root-mean-square errors (RMSE; in kg m^{-2}) of TCWV forecasts from all experiments from verification against operational model.

Whether for addition or denial experiments, the impact of SSM/I observations on TCWV forecast scores is always positive and slightly larger for clear-sky than for rain-affected observations. This is consistent with observing system experiments that have been performed over the continental United States. Lopez and Bauer (2007) replaced moisture-sensitive conventional and satellite observations with TCWV retrievals based on NEXRAD rainfall observations and found significant improvement in both moisture analysis and forecast.

In Figure 4, the gap between TCWV root-mean-square forecast errors (RMSE) from *BL* and $BL + RAIN$ or $BL + CLEAR$ is rather substantial and amounts to about 1 day over the first 48 hours. This means that the skill of both $BL + RAIN$ and $BL + CLEAR$ at day 2 is as high as for *BL* at day 1. The combined effect of $BL + RAIN + CLEAR$ adds another 3 hours of skill. In the denial experiments the loss of skill from withdrawing SSM/I data on TCWV forecast skill is visible but not significant in global terms beyond 24-48 hours.

Figure 5 breaks up the global errors into zonal cross-sections and displays relative RMSE with respect to the worst case, i.e. *BL*. This illustrates the improvement of all other experiments with respect to a poor system after 1 and 3 days, respectively. It becomes obvious, that the strongest impact on forecast skill from adding clear-sky or rain-affected observations is in the Tropics roughly between ± 30 degrees latitude but also in the Southern hemisphere where the predominance of oceans allows the assimilation of much SSM/I data. Here, the error reduction with respect to *BL* amounts to 30% for day-1 and reduces to 10% and a less strong zonal gradient at day-3. In the Tropics, both $BL + RAIN$ and $BL + CLEAR$ perform similarly while $BL + CLEAR$ shows a stronger improvement at higher latitudes. In the denial experiments, withdrawing clear-sky observation always reduces TCWV day-1 forecast skill more (5%) than withdrawing rain-affected observations; however in the tropics their effect is rather similar. The effect is still noticeable at day-3 but rather insignificant.

If the forecast errors are stratified by level and latitude bands for relative humidity (Figure 6) and vector winds *VW* (Figure 7) the following picture emerges:

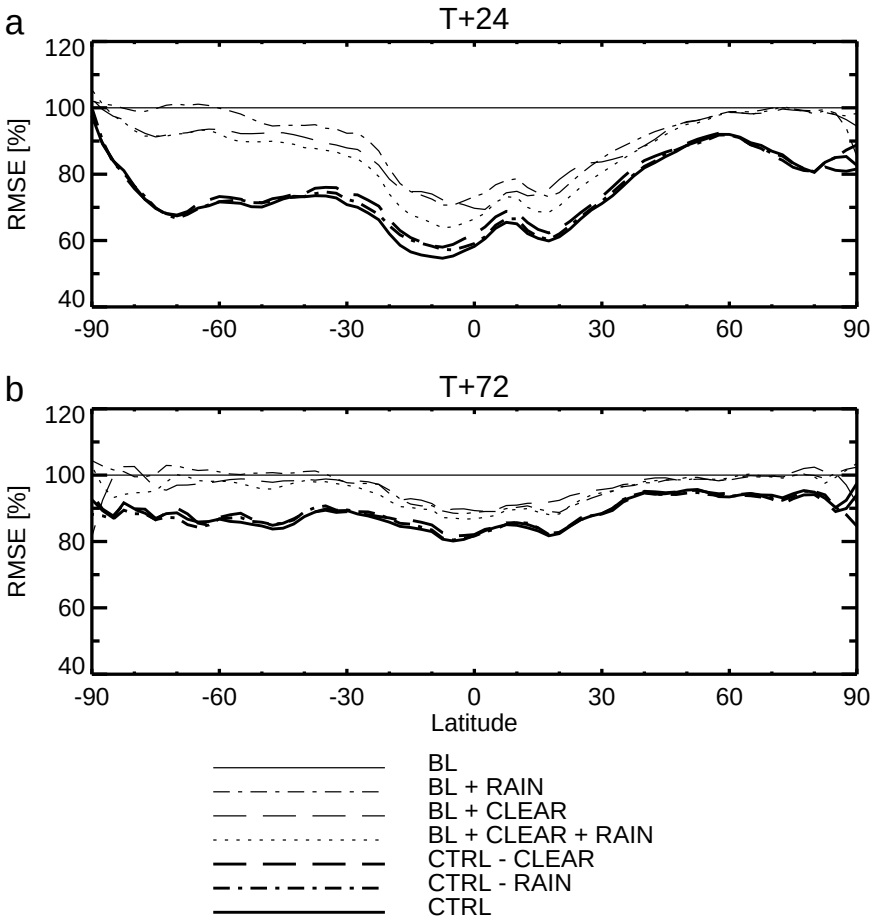

Figure 5: Relative root-mean-square errors (RMSE; in % compared to BL=100%) of TCWV forecasts from all experiments after 24 (a) and 72 hours (b).

1. The impact of data addition/denial experiments is much larger in the tropics (here between ± 20 degrees latitude). Outside the tropics, the impact is rather small but stronger in the Southern than in the Northern hemisphere. This is due to the better constraint of the dynamics and humidity analysis by conventional observations over land surfaces in the North, as indicated by the small gap between BL and $CTRL$ forecast scores.

2. For R (Figure 6), $BL + RAIN$ performs better than $BL + CLEAR$ at 200 and 500 hPa while they are very similar at 700 and 1000 hPa. This suggests that the stronger vertical extent between boundary layer and tropopause of the impact in $BL + RAIN$ through the involvement of convection is signifi cant. The vertical distribution of $BL + CLEAR$ will be more affected by the shape of the background moisture errors (which peak between 700 and 950 hPa) than the moist physics because the observations are located in areas away from saturation.

3. The combined effect in $BL + RAIN + CLEAR$ is always equal to or better than either $BL + CLEAR$ or $BL + RAIN$. This indicates that both observation types are mostly complementary despite oppostion of both contributions in smaller areas like the southern sub-tropics (Figure 1). This improvement increases towards the surface.

4. For VW (Figure 7), a similar behaviour as for R can be observed. The improvement from BL to $BL +$

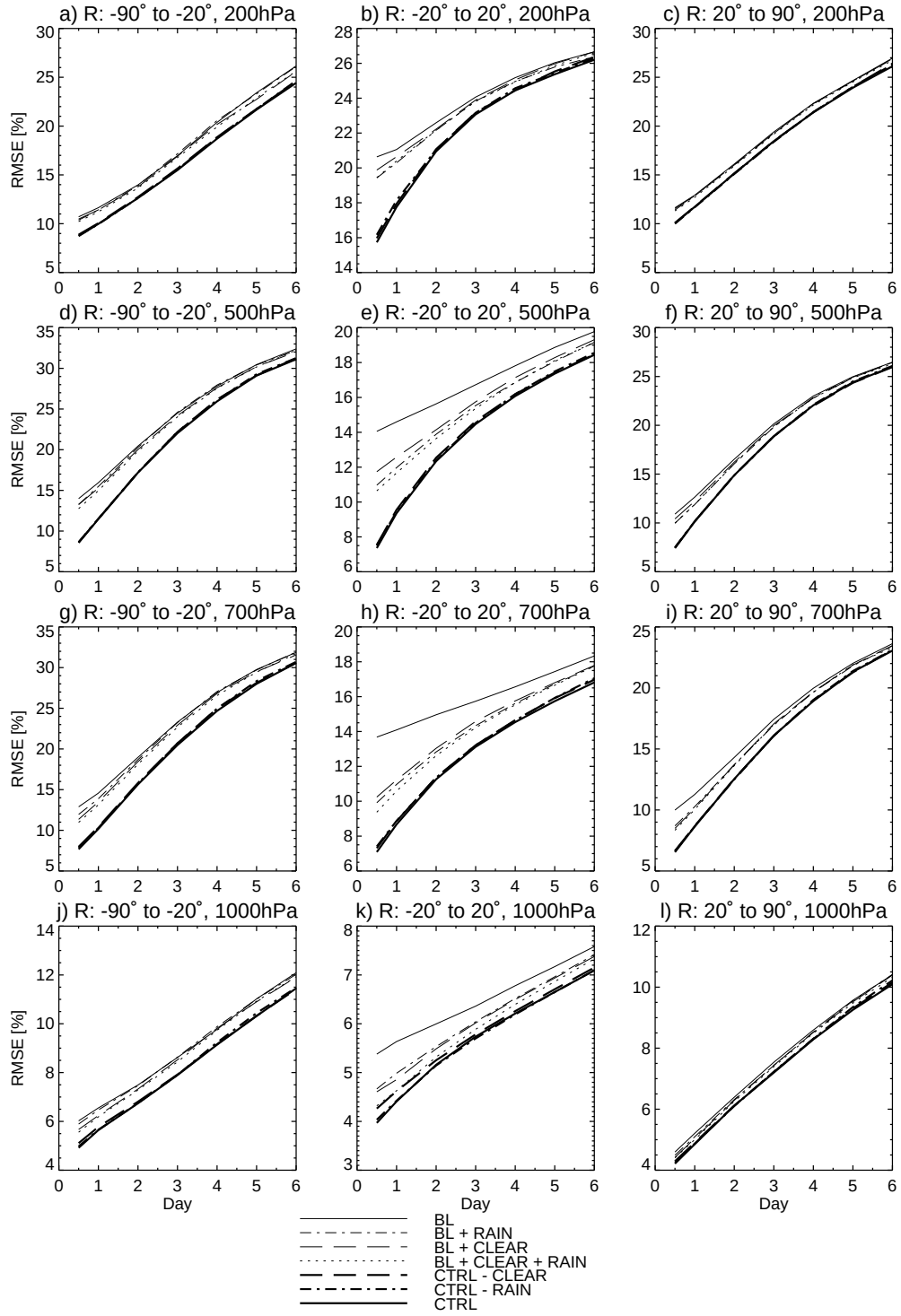

Figure 6: Root-mean-square errors (RMSE; in %) of relative humidity (R) forecasts from all experiments stratified by level at 200, 500, 700, 1000 hPa (from top to bottom) and by latitude between Southern hemisphere, Tropics, and Northern hemisphere (from left to right) from verification against operational model.

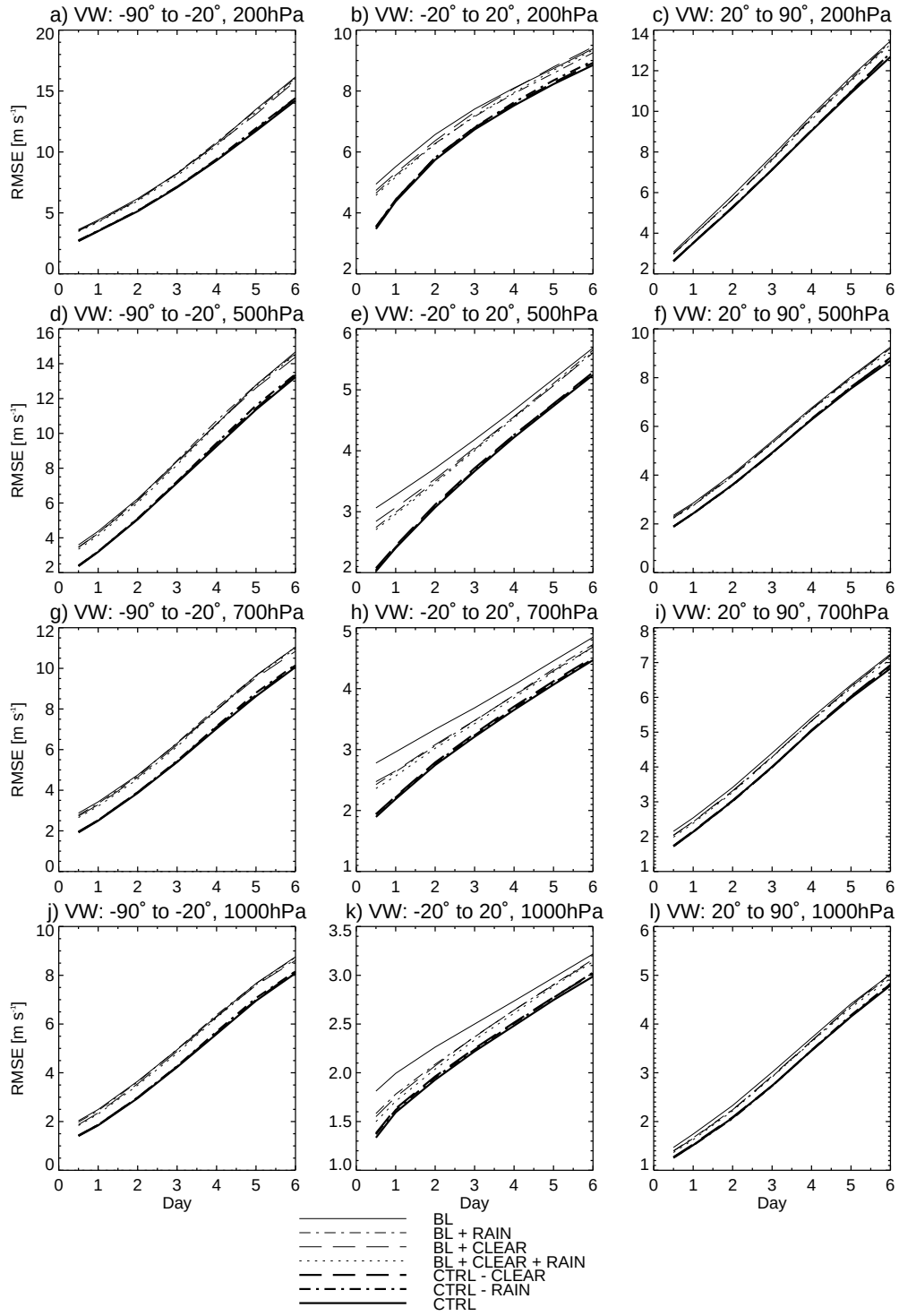

Figure 7: As Figure 6 for vector wind in ms^{-1} (VW).

CLEAR/*BL* + *RAIN* is still quite large demonstrating that moisture observations can have a direct and signifi cant impact on wind forecasts. As for *TCWV* and *R*, the gap between *BL* and *BL* + *CLEAR*/*BL* + *RAIN* is about 1 day and more over the fi rst 48 hours. The gap is slightly reduced but signifi cant for the

BL-related experiments while it disappears for the *CTRL*-related experiments after day 3. Obviously, this relates to the length of memory of the full system with respect to moisture observations at initial time.

4 Conclusions

This paper presents the results from carefully performed Observing System Experiments with the current ECMWF data assimilation and modeling system. The experiments were aimed at quantifying the impact of SSM/I observations sensitive to clear-sky moisture, to near-surface windspeed and, most importantly, to clouds and precipitation on both analysis and forecast quality. The assimilation of rain-affected observations was implemented in operations in June 2005 and can be considered a major accomplishment for adding observations in otherwise data-sparse regions. The experiments were set up such that both clear-sky and rain-affected observations were either added to a poor baseline observing system configuration or withdrawn from the full system. Experiment duration was 10 weeks of which the first 14 days were excluded from the evaluation to allow for model spin-up.

The basic impact on the analysis is demonstrated by adding data to the baseline configuration. Both clear-sky and rain-affected observations account for the bulk correction of moisture in the analysis because their combined effect almost entirely compensates for the humidity errors contained in the baseline when it is compared to the full system.

The impact of data denial and addition on forecast skill is significant. In terms of total column water vapour, SSM/I data adds 1 day of skill over the first 48 hours. In the Tropics, the rain-affected data contributes more skill to the moisture forecast than the clear-sky data for levels above 700 hPa while it is similar to clear-sky data below. In the Northern and Southern hemisphere the effect is generally weaker and slightly in favour of clear-sky observations. A similar performance can be seen with respect to wind vector forecast skill that indicates the connection between moisture analysis and vertical motions in the Tropics.

These results clearly demonstrate the important and unique role of microwave imager data in modern numerical weather prediction systems. Further developments for optimizing this observing system will be devoted to extending data coverage by adding other imagers such as the Special Sensor Microwave Imager Sounder (SSMIS), Advanced Microwave Scanning Radiometer (AMSR-E) and the Tropical Rainfall Measuring Mission (TRMM) Microwave Imager (TMI) as well as by exploiting the use of combined microwave imager-sounder data over land surfaces. This study also served as demonstration of the beneficial impact of rain-affected radiance data in modern forecasting systems and supports the requirement of adding data in areas where current systems have been only weakly constrained by observations.

The experiments have been performed with the latest version of the ECMWF modelling and data assimilation system and the denial experiments withdraw SSM/I data from a suite of about 30 different satellite instruments. Therefore, the results have to be interpreted in this context when compared to those published by Bengtsson and Hodges (2005) and Andersson et al. (2007). Due to the limited interaction between moisture and other control variables in the analysis system, it was important to employ AMSU-A radiance observations from NOAA-16 in our baseline experiment to adjust the large-scale dynamic structures in the atmosphere. Otherwise, moisture observations alone may not show beneficial impact in data sparse areas like the Southern hemisphere. Hence, the baseline-related experiments clearly show the strong contribution of SSM/I observations to forecast skill and the impact of humidity observations on forecast winds in the Tropics well into the medium range.

In the data denial experiments, the impact of SSM/I data withrawal from the full observing system was found to be mainly relevant in the tropics even though its magnitude was smaller and most effective over the first 1-2 days. This is partly explained by the amount of other satellite observations, that are sensitive to moisture,

present in all denial and control experiments and the shorter memory of moisture forcing through the effective removal by precipitation and evaporation.

Acknowledgements

This study was mainly funded by the European Organisation for the Exploitation of Meteorological Satellites (EUMETSAT) through contract EUM/MET/SOW/04/0290 and the EUMETSAT fellowship programme.

References

Andersson, E., R. Dumelow, H. Huang, J.-N. Thépaut and A. Simmons, 2004: Space/Terrestrial Link - Outline Study proposal for consideration by EUCOS management (available at EUCOS secretariat).

Andersson, E., P. Bauer, A. Beljaars, F. Chevallier, E. Holm, M. Janiskovà, P. Kallberg, G. Kelly, P. Lopez, A. McNally, E. Moreau, A. Simmons and J.-N. Thépaut, 2005: Assimilation and Modelling of the Hydrological Cycle. *Bull. Amer. Meteorol. Soc.*, **86**, 387–402.

Andersson, E., E. Hólm, P. Bauer, A. Beljaars, G.A. Kelly, A.P. McNally, A.J. Simmons, and J.-N. Thépaut, 2007: Analysis and forecast impact of the main humidity observing system. *Q. J. Roy. Meteor. Soc.*, in press.

Auligné, T., A.P. McNally, and D.P. Dee, 2007: Adaptive bias correction for satellite data in a numerical weather prediction system. *Q. J. Roy. Meteor. Soc.*, **133**, 631-642.

Bauer, P., G. Kelly, and E. Andersson, 2002: SSM/I radiance assimilation at ECMWF. Proc. ECMWF/GEWEX Workshop on Humidity Analysis, Reading, United Kingdom, ECMWF, 167-175. Available from European Centre for Medium-Range Weather Forecasts, Shinfi eld Park, Reading RG2 9AX, United Kingdom.

Bauer, P., P. Lopez, A. Benedetti, D. Salmond, and E. Moreau, 2006a: Implementation of 1D+4D-Var assimilation of precipitation affected microwave radiances at ECMWF, Part I: 1D-Var. *Q. J. Roy. Meteor. Soc.*, **132**, 2277–2306.

Bauer, P., P. Lopez, A. Benedetti, D. Salmond, S. Saarinen and M. Bonazzola, 2006b: Implementation of 1D+4D-Var assimilation of precipitation affected microwave radiances at ECMWF, Part II: 4D-Var. *Q. J. Roy. Meteor. Soc.*, **132**, 2307–2332.

Bengtsson, L. and K.I. Hodges, 2005: On the impact of humidity observations in numerical weather prediction. *Tellus*, **57A**, 701-708.

Courtier, P., J.-N. Thépaut, and A. Hollingsworth, 1994: A strategy for operational implementation of 4D-Var using an incremental approach. *Q. J. Roy. Meteor. Soc.*, **120**, 1367–1387.

Dee, D.P., 2005: Bias and data assimilation, *Q. J. Roy. Meteor. Soc.*, **131**, 3323–3343.

Errico, R., P. Bauer, and J.-F. Mahfouf, 2007: Assimilation of cloud and precipitation data: Current issues and future prospects. *J. Atmos. Sci.*, accepted.

Gérard, E. and R. Saunders, 1999: Four-dimensional variational assimilation of Special Sensor Microwave/Imager total column water vapour in the ECMWF model. *Quart. J. Roy. Meteorol. Soc.*, **125**, 3077-3102.

Haseler, J., 2004: The early-delivery suite. *ECMWF Technical Memorandum*, **No. 454**, 35 pp. Available from European Centre for Medium-Range Weather Forecasts, Shinfield Park, Reading RG2 9AX, United Kingdom.

Heckley, W.A., G. Kelly, and M. Tiedtke, 1990: On the use of satellite-derived heating rates for data assimilation within the tropics. *Mon. Wea. Rev.*, **118**, 1743–1757.

Kållberg, P., P. Berrisford, B. Hoskins, A. Simmons, S. Uppala, S. Lamy-Thépaut and R. Hine, 2005: ECMWF Re-Analysis: 19. ERA-40 Atlas. Available from ECMWF, Shinfield Park, Reading RG2 9AX, UK, pp. 191.

Krishnamurti, T.N., K. Ingles, S. Cooke, T. Kitade, and R. Pash, 1984: Details of low-latitude medium-range numerical weather prediction model using a global spectral model. Part 2: Effects of orography and physical initialization. *J. Meteor. Soc. Japan*, **62**, 613–648.

Krishnamurti, T.N., and H.S. Bedi, 1996: A brief review of physical initialization. *Meteor. Atmos. Phys.*, **60**, 137–142.

Lopez, P. and P. Bauer, 2007: 1D+4D-Var assimilation of NCEP Stage IV radar and gauge hourly precipitation data. *Mon. Wea. Rev.*, in press.

Phalippou, L., 1996: Variational retrieval of humidity profile, wind speed and cloud liquid-water path with the SSM/I: Potential for numerical weather prediction. *Quart. J. Roy. Meteorol. Soc*. **122**, 327-355.

Puri, K. and M.J. Miller, 1990: The use of satellite data in the specification of convective heating for diabatic initialization and moisture adjustment in numerical weather prediction models. *Mon. Wea. Rev.*, **118**, 67–93.

Rabier, F., A. McNally, E. Andersson, P. Courtier, P. Unden, J. Eyre, A. Hollingsworth, and F. Bouttier, 1998: The ECMWF implementation of three-dimensional variational assimilation (3D-Var):. II: Structure functions. *Q. J. Roy. Meteor. Soc.*, **124**, 1809–1829.

Trémolet, Y., 2004: Diagnostics of linear and incremental approximations in 4D-Var. *Q. J. Roy. Meteor. Soc.*, **130**, 2233-2251.

Tsuyuki, T., 1997: Variational data assimilation ibn the Tropics using precipitation data. Part III: Assimilation of SSM/I precipitation rates. *Mon. Wea. Rev.*, **125**, 1447–1464.

Uppala, S.M., and co-authors, 2005: The ERA-40 re-analysis, *Q. J. Roy. Meteor. Soc.*, **131**, 2961–3012.

Zupanski D., and F. Mesinger, 1995: Four-dimensional variational assimilation of precipitation data. *Mon. Wea. Rev.*, **123**, 1112–1127.

Zou, X., and Y.-H. Kuo, 1996: Rainfall assimilation through an optimal control of initial and boundary conditions in a limited-area mesoscale model. *Mon. Wea. Rev.*, **124**, 2859–2882.